



Parallelization of a 3D FDTD code and physics studies of EC heating and current drive in fusion plasmas

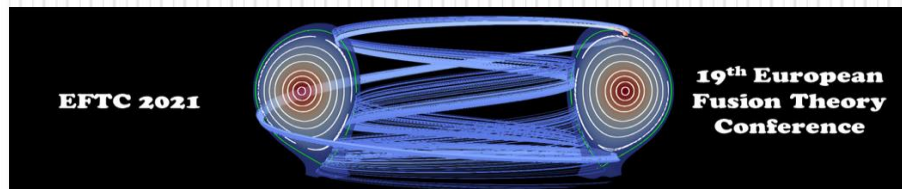
C. Tsironis

A. Papadopoulos

M. Martone

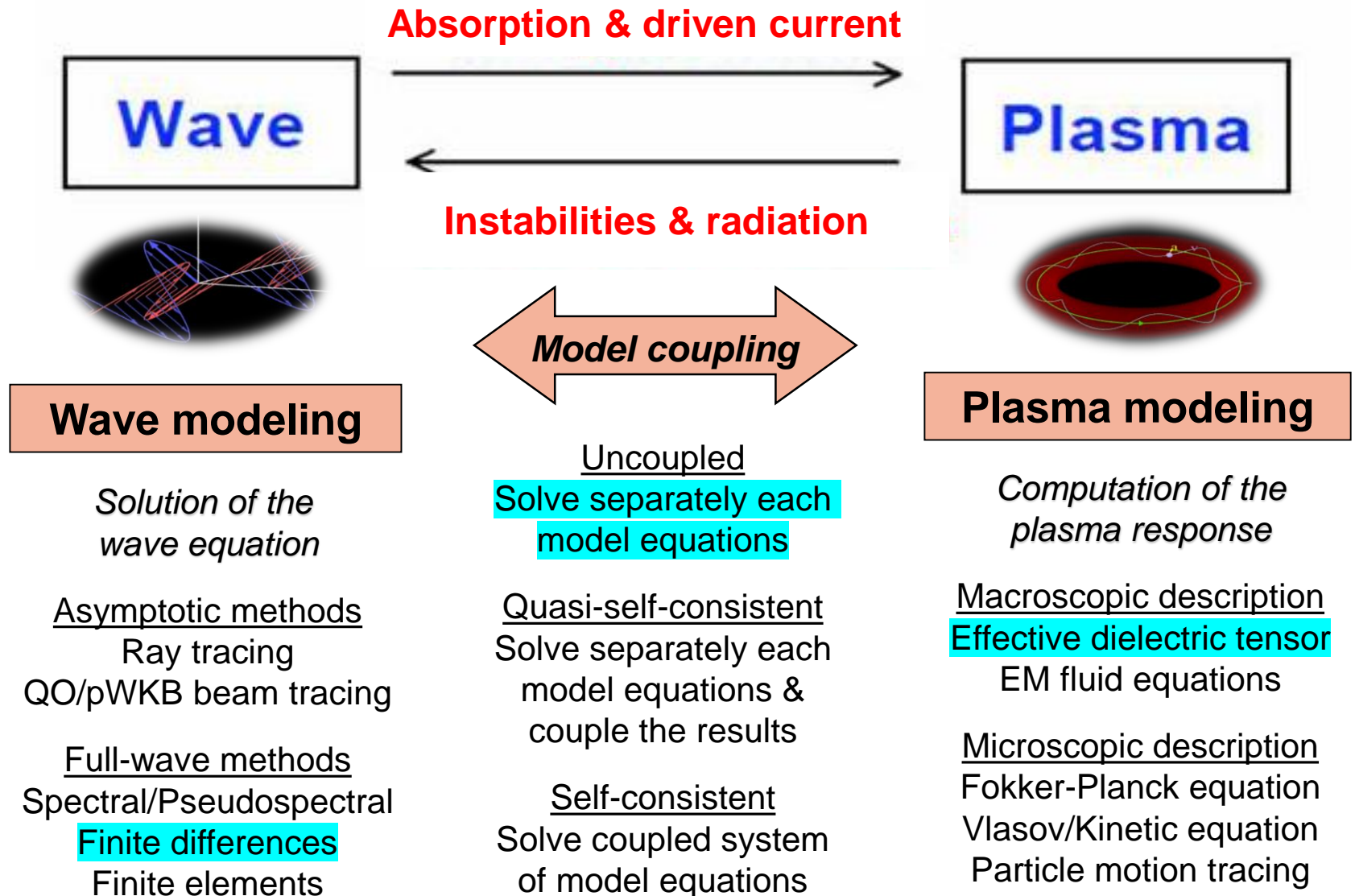


*School of Electrical and Computer Engineering
National Technical University of Athens
Athens, Greece*



CONSORZIO RFX
Ricerca Formazione Innovazione

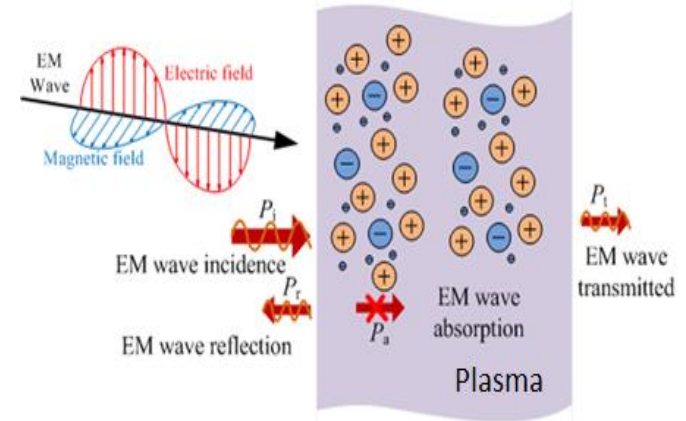
The wave – plasma physical system



EC wave (beam) propagation in plasma

■ The wave equation describes EM propagation in plasmas

- Full problem solution: Extremely hard!
 - Wave equation → Inhomogeneous PDE
 - Dynamic equation for plasma current?
- Numerical solution of PDEs?
 - Resource-demanding code execution!!!
 - Spatial grid progressing onto temporal grid



■ Approximate solution given by asymptotic methods

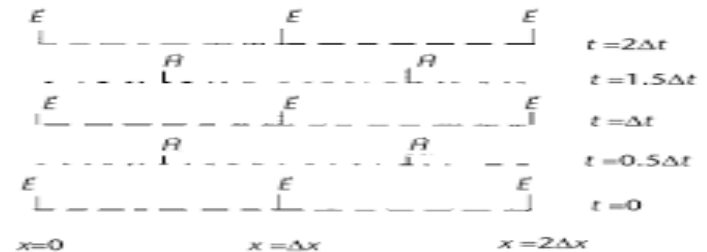
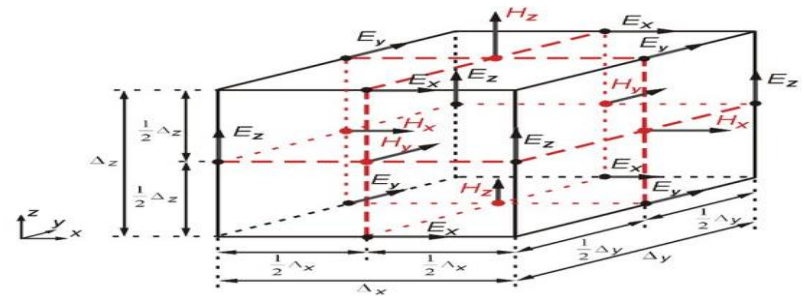
- Ray tracing (geometrical optics): Propagation described in analogy with particle dynamics (momentum → wave-vector, energy → frequency).
- Quasi-optical beam tracing: Wave-vector generalized to include an imaginary part related to the transverse beam electric field profile.
- Paraxial WKB beam tracing: Beam trajectory identified as a GO ray & described by scalar functions for the amplitude, width and curvature.

■ Advanced EC codes are based on asymptotic methods

- Approximations??? Plasma stationarity, weakly-inhomogeneous plasma, cold plasma dispersion, linear & weakly-relativistic kinetics.

Need for full-wave methods???

- The approximations present in asymptotic methods break down in several cases of practical interest:
 - ① $\lambda \ll \max(\text{inhomogeneity scale})$ • ② $T \ll \max(\text{transients scale})$
 - Hot plasma dispersion, mode conversion, steep plasma gradients etc.
 - Alternative → Full-wave methods (albeit computationally expensive...)
- Option: Finite Difference Time Domain (FDTD) method
 - Maxwell's curl equations transformed to *central finite-differences*.
 - Spatial grid: Placement of the electric & magnetic field vectors on *interlinked contours* in order to have Maxwell's divergence equations as *valid by identity*.
 - Temporal grid: The electric field is computed at a given time instant, then the magnetic field is computed at the next time instant and so on (*leapfrog integration scheme*).



The code *RFFW* (Radio Frequency Full Wave)

- **Numerical FDTD solver for the propagation of EM waves with generic electric field profile in arbitrary plasmas:**
 - *1D/2D/3D propagation grid* (optimal choice ↔ based on the problem)
 - *Scattered field formalism* (separation of incident & response EM field)
 - *Cold/Warm/Hot plasma dielectric response* (time-domain current density equation vs frequency-domain “effective” dielectric tensor)
 - *Arbitrary plasma geometry* (fusion device equilibria, space plasmas, ...)
 - *Generic wave/beam geometry* (plane wave, Gaussian beam, ...)
 - *Various boundary condition schemes* (conducting, absorbing,...)
- **Example: Plane wave @ 1D hot plasma (AUG parameters)**



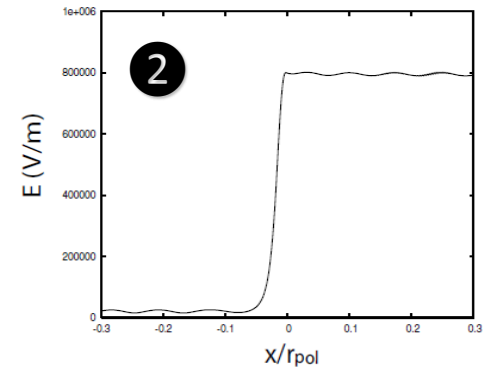
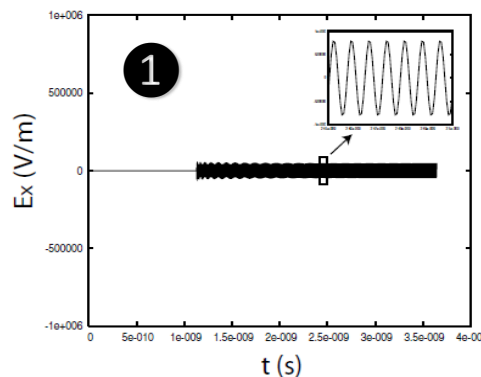
ASDEX Upgrade

$R_{\text{tor}} = 1.65 \text{ m}$ • $r_{\text{pol}} = 0.6 \text{ m}$
 $B_{\text{tor}}(\mathbf{x} = \mathbf{0}) = 2.5 \text{ T}$
 $n_e = [1.4, 1.6] \cdot 10^{13} \text{ cm}^{-3}$
 $T_e = [0.2, 2] \text{ KeV}$
 $f = 140 \text{ GHz (mode X2)}$
 $P_0 = 1 \text{ MW}$

$$\omega_{ce}(x) = \frac{\omega_{ce}|_{x=0}}{1 + \frac{x}{r_{\text{tor}}}}$$

$$\omega_{pe}^2(x) = \omega_{pe}^2|_{x=0} + (\omega_{pe}^2|_{x=r_{\text{pol}}} - \omega_{pe}^2|_{x=0}) \left(\frac{x}{r_{\text{pol}}}\right)^2$$

$$v_{te}^2(x) = v_{te}^2|_{x=0} + (v_{te}^2|_{x=r_{\text{pol}}} - v_{te}^2|_{x=0}) \left(\frac{x}{r_{\text{pol}}}\right)^2$$



- 1 Dynamic evolution of the x-component of the electric field •
 2 Spatial profile of the electric field amplitude

Inside RFFW: FDTD formalism

■ Scattered field formalism: Separation of EM wave field

□ $\mathbf{E}_t = \mathbf{E}_i + \mathbf{E}_s$ [Total field] = [Incident field] + [Scattered field]

- Incident field: EM field as in absence of the medium (i.e. in vacuum)
- Scattered field: Generated by the medium in response to incident field

■ Discretized FDTD equations:

$$\nabla \times \mathbf{E}_s = -\mu_0 \frac{\partial \mathbf{H}_s}{\partial t} \quad \longrightarrow \quad H_{qs}|_{i,j,k}^{n+1/2} = H_{qs}|_{i,j,k}^{n-1/2} - \frac{\Delta t}{\mu_0 \Delta l} \psi_q [\mathbf{E}_s|_{i,j,k}^n]$$

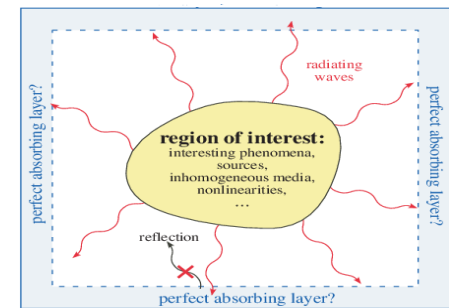
$$\nabla \times \mathbf{H}_s = \bar{\sigma} \mathbf{E}_s + \bar{\epsilon} \frac{\partial \mathbf{E}_s}{\partial t} + \bar{\sigma} \mathbf{E}_i + \left(\bar{\epsilon} - \epsilon_0 \bar{I} \right) \frac{\partial \mathbf{E}_i}{\partial t} \quad \longrightarrow \quad E_{qs}|_{i,j,k}^{n+1} = \sum_{l=1}^3 \sum_{m=1}^3 \alpha_{ql}|_{i,j,k} \left\{ \tau_{lm}|_{i,j,k} E_{ms}|_{i,j,k}^n + \psi_q [\mathbf{H}_s|_{i,j,k}^{n+1/2}] - \sigma_{lm}|_{i,j,k} E_{mi}|_{i,j,k}^{n+1/2} - (\epsilon_{lm}|_{i,j,k} - \epsilon_0 \delta_{lm}) \frac{\partial E_{mi}}{\partial t} |_{i,j,k}^{n+1/2} \right\}$$

■ Boundary conditions:

- Provision of the “missing” nearest-neighbour grid components for the boundary EM field evaluation.
- Several options of FDTD BC schemes:

- Outer radiating $\longrightarrow E_z|_0^{n+1} = -E_z|_1^{n-1} + \frac{c\Delta t - \Delta x}{c\Delta t + \Delta x} (E_z|_1^{n+1} + E_z|_0^{n-1}) + \frac{2\Delta x}{c\Delta t + \Delta x} (E_z|_0^n + E_z|_1^n)$

- Absorbing boundary $\longrightarrow \frac{1}{\kappa_y} \frac{\partial E_z^{sc}}{\partial y} - \frac{1}{\kappa_z} \frac{\partial E_y^{sc}}{\partial z} + \psi_{H_{xy}}^{sc} - \psi_{H_{xz}}^{sc} = -\mu \frac{\partial H_z^{sc}}{\partial t} - (\mu - \mu_0) \frac{\partial H_z^{in}}{\partial t} + \psi_{E_{xy}}^{sc} |_{i+\frac{1}{2},j,k}^{n+\frac{1}{2}} = b_{yj} \psi_{E_{xy}}^{sc} |_{i+\frac{1}{2},j,k}^{n-\frac{1}{2}} + c_{yj} \frac{\partial H_z^{sc}}{\partial y} |_{i+\frac{1}{2},j,k}^{n+\frac{1}{2}}$



Inside RFFW: Medium formalism

- Availability of different response models to EM waves depending on the plasma kinetic state:

Cold plasma

Non-relativistic, inhomogeneous, anisotropic & linear plasma current equation in time domain

$$\frac{\partial \mathbf{J}}{\partial t} = \epsilon_0 \omega_p^2(\mathbf{r}, t) \mathbf{E} + \omega_c \times \mathbf{J}$$

Hot plasma

Weakly-relativistic, inhomogeneous, anisotropic & linear plasma dielectric tensor in frequency domain

$$\tilde{\epsilon} = \tilde{\mathbf{I}} + \frac{\omega_{pe}^2}{\omega} \sum_{l=-\infty}^{\infty} \int \frac{\frac{1}{\gamma p} \frac{df_0}{dp}}{\omega - k_{||} v_{||} - \frac{l\omega_{ce}}{\gamma}} \begin{bmatrix} \frac{l^2}{\beta_J^2} J_l^2 p_{\perp}^2 & i \frac{l}{\beta_J} J_l J_l' p_{\perp}^2 & \frac{l}{\beta_J} J_l^2 p_{||} p_{\perp} \\ -i \frac{l}{\beta_J} J_l J_l' p_{\perp}^2 & J_l'^2 p_{\perp}^2 & -i J_l J_l' p_{||} p_{\perp} \\ \frac{l}{\beta_J} J_l^2 p_{||} p_{\perp} & i J_l J_l' p_{||} p_{\perp} & J_l'^2 p_{||}^2 \end{bmatrix} d^3 p$$

- Axisymmetric model for the magnetic field:

$$\mathbf{B} = B_t \mathbf{e}_{\phi} + B_p \mathbf{e}_{\theta}$$

$$B_t(r, \theta) = \frac{B_0}{1 + \epsilon_A(r) \cos \theta} \quad B_p(r, \theta) = \frac{\epsilon_A(r)}{q(r)} B_t(r)$$

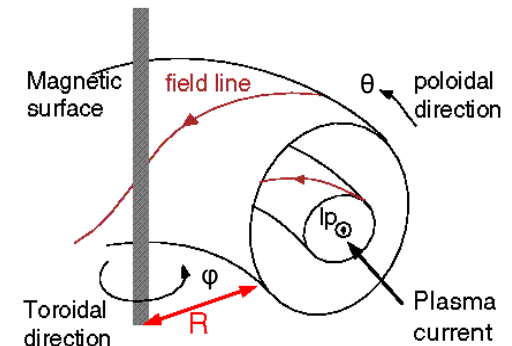
- Profile parameters: Aspect ratio & safety factor

- Inverse aspect ratio: $\epsilon_A(r) = r/R_0$

- q-profile: $q(r) = q_{\min} + (q_{\max} - q_{\min}) \cdot r^2/a^2$

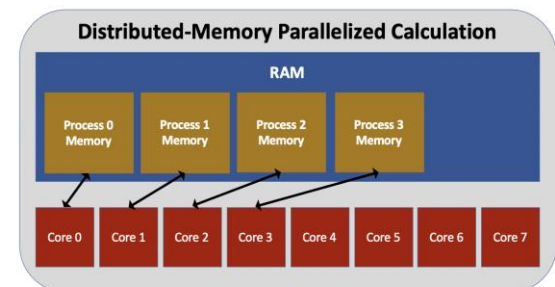
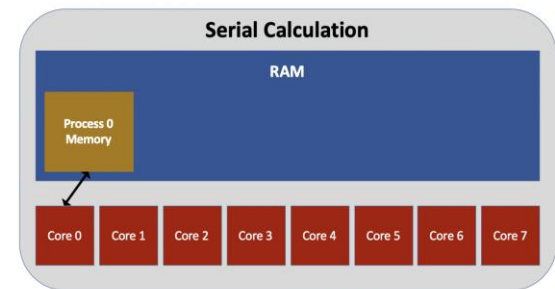
- Inclusion of non-axisymmetric perturbations (e.g. magnetic islands):

- \mathbf{B} defined by flux functions (Clebsch formalism) $\Rightarrow \mathbf{B} = \nabla \psi_t \times \nabla \theta - \nabla \psi_p \times \nabla \phi$



Need for code parallelization!!!

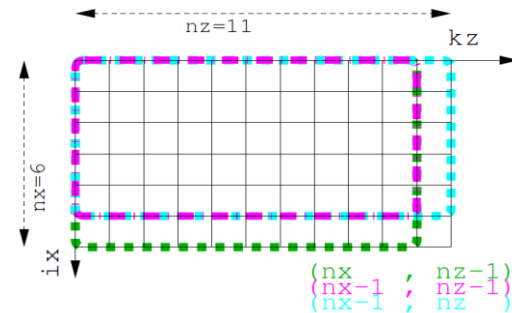
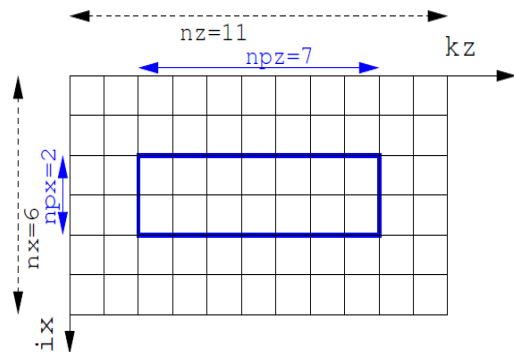
- **The serial version of RFFW comes with very important computational limitations!**
 - Non-fusion plasma: Realistic simulation times & memory requirements.
 - Plasma density \ll Average densities of medium-sized tokamaks.
 - Plasma dimensions \ll Average medium-size tokamaks poloidal radius.
 - Without multi-core exploitation & distributed memory parallelism, the code cannot handle problems that involve ITER-sized plasmas.
 - Cases relevant to fusion: CPU time \sim 20-180 days, RAM \sim 32-96 GB.
- **Apply hybrid parallelization scheme (coordinated by EUROfusion HLST)**
 - *Analysis of grids type & code variables*
 - Staggered vs collocated grids?
 - Annotate to-be-affected code variables.
 - *OpenMP workload partitioning*
 - Introduction of shared memory constructs.
 - *MPI data & workload partitioning*
 - Based on ghost & boundary cell exchange communication primitives.
 - Implemented in separate code module.



Hybrid parallelization: Design & OpenMP

■ Step #1: Identify grids type & the impacted variables

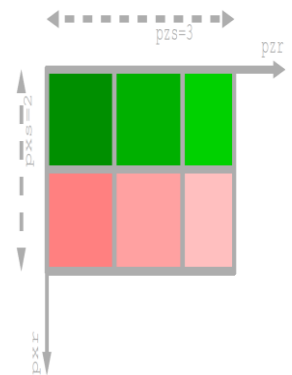
- RFFW uses *staggered* grids → Advantage!!!
 - Scalar and vector variable computations may be “coupled”.
 - Avoidance of singularities & convergence problems is easier.
- Some variables & indices have to be pertained to the local domain only.



■ Step #2: OpenMP primitives

- Different portions of the grid space get updated *in parallel*.
 - Many threads per array copy.
- Introduce **thread local (private)** variables where required.
 - Declared bounds remain **global**

```
!$OMP PARALLEL DEFAULT(SHARED) PRIVATE
(ix,kz,...,exs_interp,...)
...
!$OMP DO SCHEDULE (STATIC)
eysloopz: do kz=2,nz-1
!kz set by OpenMP on each thread
eysloopx: do ix=2,nx-1
!ix ranging 2 to nx-1
...
eys(ix,kz)=exs_interp...+eys(ix,kz)*...
...
end do eysloopx
end do eysloopz
!$OMP END DO
...
!$OMP END PARALLEL
```



Hybrid parallelization: MPI

■ Step #3a: MPI data management

□ Transition from *global* to *local* structures:

- Introduction of process *local* subdomains (subsets of the *global* one).
- Replace *local* loop indices with *global* ones (in order to optimize loop iterations).

EXAMPLE

```

do kz=npz_1,npz_2
do ix=npx_1,npx_2
...
end do
end do
    
```

➔

```

do kz=lpz_1,lpz_2
do ix=lpx_1,lpx_2
...
end do
end do
    
```

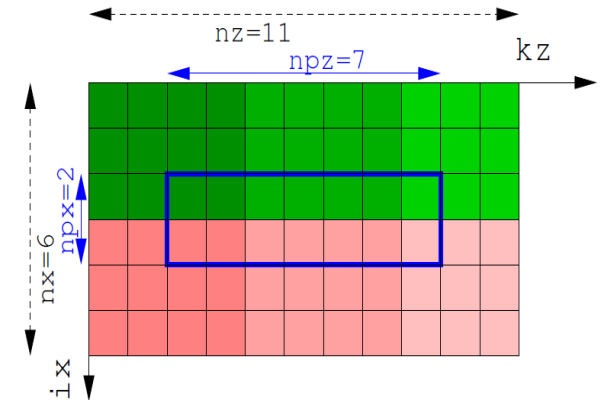
□ Optimize boundary condition routines:

- Retain code via preprocessor *conditionals*.

EXAMPLE

```

orbcexszi: do ix=lx_1,lxm_2,1
FWTOR_IF_Z_1 exs(ix,1)=exsz_1(ix,2)+...
FWTOR_IF_Z_2 exs(ix,nz)=exsz_1(ix,3)+...
end do orbcexszi
    
```



■ Step #3b: MPI communication

□ Ghost/boundary cell exchanges.

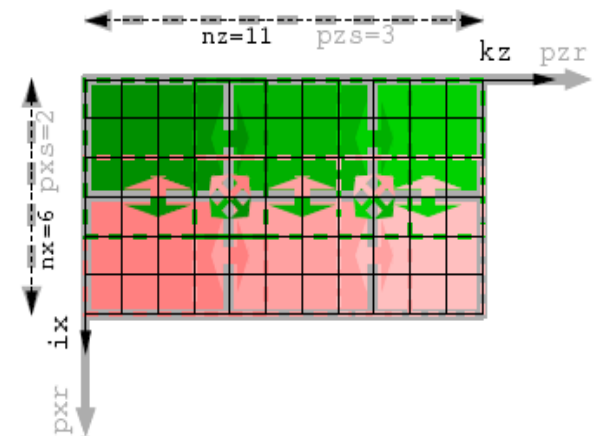
- Required in finite difference schemes at the vicinity of the grid boundaries.

EXAMPLE

```

Problem: When e.g. pxr=1.AND.ix=lxp_1
eysloopz: do kz=lpz_1,lzm_2
eysloopx: do ix=lxp_1,lxm_2
...
exs_interp=0.5*(exs(ix-1,kz)+exs(ix,kz))
...
end do eysloopx
end do eysloopz
    
```

- Direction: From owner task to neighbors.
- Realization with command MPI Sendrecv().



Tests for parallel code strong scaling

■ Tests performed @ HELIOS supercomputer:

- Fortran module → *intel/15.0.2.164*
- Cluster module → *oscar-modules/1.0.3 srun/1.0*
- MPI Modules → *bullxmpi/1.2.8.4 vs intelmpi/5.0.3.048*
- Studied 3 different cases (wrt grid size and number of steps to termination) by scaling MPI parallelism:
 - Case 1 → max_helios_node (7128 x 7128 cells)
 - Case 2 → 3564 x 3564 cells ([Case 1]/4)
 - Case 3 → 1782 x 1782 cells ([Case 1]/16)



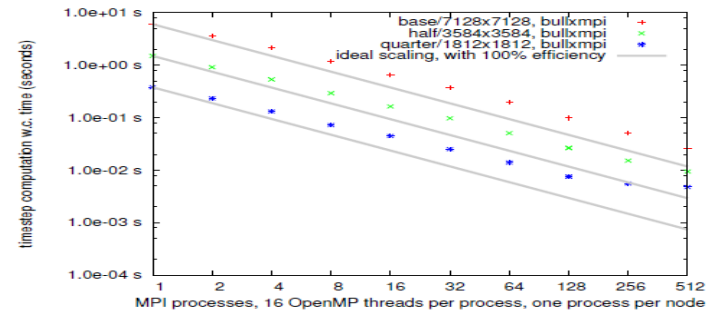
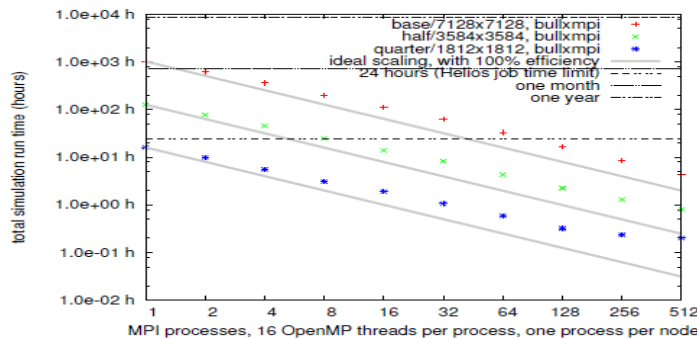
■ General assessment & comments of the results:

- Max 2500x code acceleration in the largest parallel run.
- Intel's MPI occurred to be consistently slightly faster (< 5%) than Bull's.
- OpenMP scaling of $\approx 12x$ on one node, $\approx 8x$ (of max 16x) for the largest case on many nodes.
- With message passing off, super-linear scaling is achieved.
 - Likely due to the case fitting in the last level cache.
 - In these cases, OpenMP scaling is reduced (e.g. < 8x).

Strong scaling results

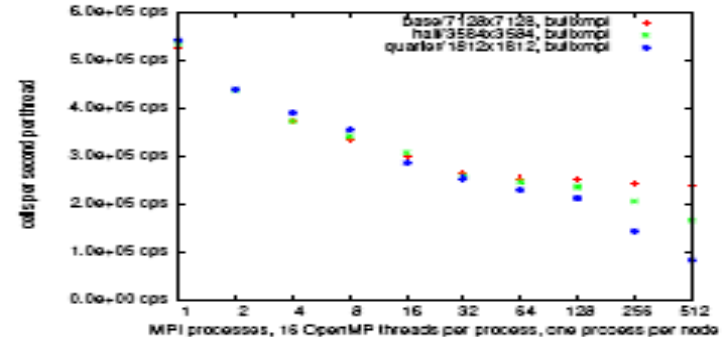
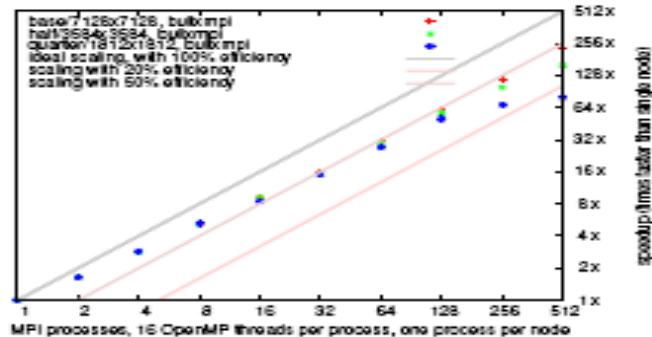
■ Total projected runtime & timestep computation time:

- max helios node case: ~380d serial; ~35d OpenMP; ~5h hybrid!!!
- Smallest case saturates @ 256nodes (113² cells/node, 28² cells/thread).



■ Speedup & scalability:

- Speedup increases wrt the grid size (in the range 80x to 200x).
- Scalability reduces as a function of the grid size.

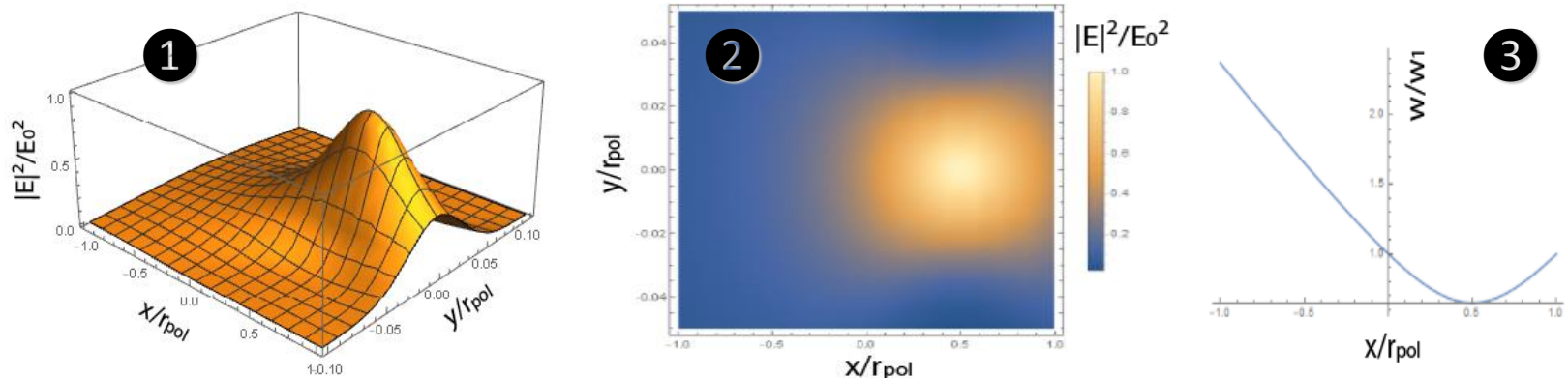


Numerical results: Cold plasma

■ 2D propagation of Gaussian beam in cold plasma @ AUG

- Device parameters: $r_{\text{tor}} = 1.65$ m, $r_{\text{pol}} = 0.6$ m, $B_0 = 2.5$ T.
- Plasma parameters: $n_e = [1.4, 1.6] \cdot 10^{13}$ cm⁻³, $T_e = 0$ KeV, $q = [1, 4]$.
- Beam parameters: $f = 140$ GHz (mode X2), $w_0 = 4$ cm, $P_0 = 1$ MW.

■ Visualization of the EC beam electric field amplitude:



- ① Surface plot of electric field amplitude • ② Electric field amplitude contours • ③ Width variation along propagation

■ Result: Focused beam propagation with no power losses

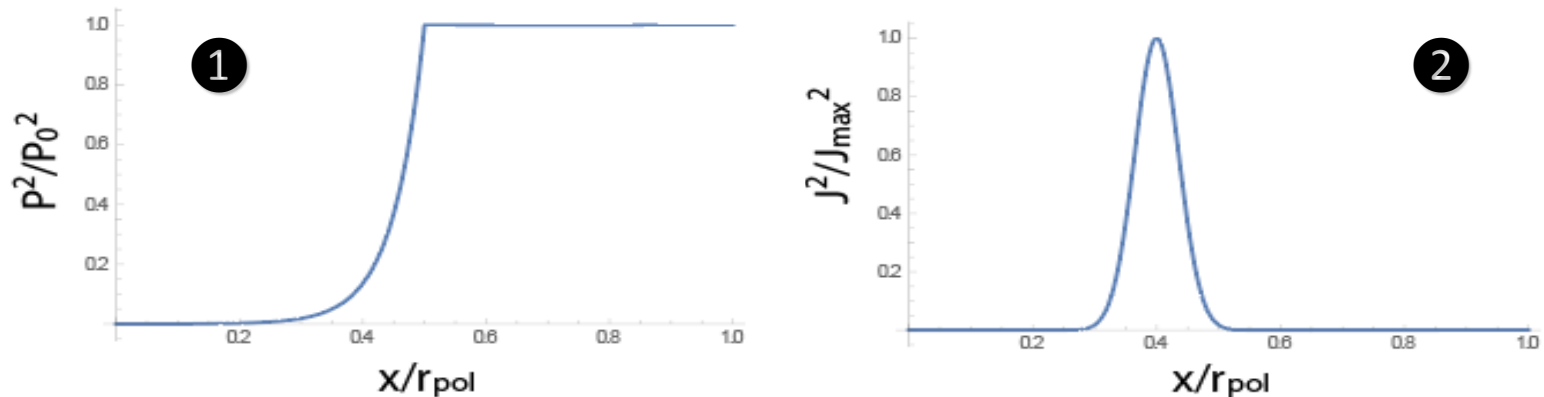
- Beam reaches its minimum width (*waist*) $\approx 0.5w_0$ near $0.5 \cdot r_{\text{pol}}$.
- Cold plasma \rightarrow No EC absorption mechanism \rightarrow No power damping.

Numerical results: Hot plasma

■ 3D propagation of plane wave in hot plasma @ TCV

- Device parameters: $r_{\text{tor}} = 0.88$ m, $r_{\text{pol}} = 0.25$ m, $B_0 = 1.44$ T.
- Plasma parameters: $n_e = [0.5, 1] \cdot 10^{13}$ cm⁻³, $T_e = [0.2, 2]$ KeV, $q = [1, 4]$.
- Wave parameters: $f = 118$ GHz (mode X3), $w_0 = \infty$, $P_0 = 0.5$ MW.

■ Plots of the EC wave power damping & generated current:



① Wave power variation along propagation • ② Spatial profile of generated electric current

■ Result: Wave damping occurs at the EC resonance layer

- Absorption begins near $0.5 \cdot r_{\text{pol}}$ and is relatively broad (width $\approx 0.2 \cdot r_{\text{pol}}$).
- Electric current is generated as a consequence of wave damping.

Improvements & future work

■ Employ frequency-domain tensor in FDTD scheme

□ Unavailability of the *hot-plasma dielectric tensor* in *time-domain*

□ *When is it inconsistent to use the frequency-domain tensor?*

■ **Answer:** When both wave spectrum & plasma response depend on \mathbf{k}

■ **OK:** Beam @ cold plasma, plane wave @ hot plasma $\tilde{\epsilon}(\mathbf{r}, t) = \frac{1}{2\pi} \int_{-\infty}^{\infty} \tilde{\epsilon}(\mathbf{r}, \omega_0) e^{-i\omega' t} d\omega' = \tilde{\epsilon}(\mathbf{r}, \omega_0) \delta(t)$

■ **Not OK (but case with practical interest...):** Beam @ warm/hot plasma

□ **Physically-consistent solution:** Convolution scheme for plasma response calculation

$$\sigma(\mathbf{k}, \omega; \mathbf{r}, t) \equiv \int d^3\mathbf{r}' \int_0^{\infty} dt' \sigma(\mathbf{r}', t'; \mathbf{r}, t) e^{-i\mathbf{k}\cdot\mathbf{r}' + i\omega t'}$$

■ Implement a fully-inhomogeneous plasma tensor

□ Based on inhomogeneous kinetic equation (*Brunner & Vaclavic 1993*)

■ Tensor operator contains the spatial derivatives of the distribution function

■ *Plasma response* → *Convolution integral of tensor with the electric field*

■ Small Larmor radius over wave field & plasma inhomogeneity

$$\begin{aligned} \epsilon_{\parallel\parallel}^{(1)} &= \epsilon_{\parallel\parallel}^{(0)} = \frac{k_p}{2\omega\Omega b_p} \left\{ \nabla_{\parallel}^2 \left[\frac{\partial}{\partial \Omega} (Z_1 - Z_{-1}) - \frac{1}{\omega} (Z_1 + Z_{-1}) \right] \right. \\ &\quad \left. + \frac{K}{2} [X_1 + X_{-1} + 4 + \lambda \frac{\Omega}{\omega} (W_1 - W_{-1})] \right\} \\ \epsilon_{\parallel\perp}^{(1)} &= -\epsilon_{\perp\parallel}^{(1)} = \frac{i}{b_p} \left\{ \nabla_{\parallel}^2 \left[B_{\parallel\parallel} + \frac{k_p}{2\omega^2 \Omega} (Z_1 - Z_{-1}) \right] \right. \\ &\quad \left. + \frac{K}{2} [X_1 - X_{-1} + \lambda \frac{\Omega}{\omega} (W_1 + W_{-1} - \frac{2}{\lambda})] \right\} \\ \epsilon_{\perp\perp}^{(1)} &= \frac{1}{\Omega b_p} \left(\nabla_{\perp}^2 \frac{\partial \tilde{Z}_0}{\partial k_p} \right) + 2K \left(\frac{\omega}{k_p v_{th}} \right)^2 \left[\lambda (Y_0 - Y_0^*) - \left(\frac{\omega}{k_p v_{th}} \right)^2 Y_0 + 1 \right] \end{aligned}$$

$$\begin{aligned} \epsilon_{\parallel\parallel}^{(1)} &= B_{\parallel\parallel} (\nabla_p + \beta_{\parallel n}) + i B_{\parallel\parallel} (\nabla_n - \beta_{\parallel b}) \\ &\quad + \frac{2}{\Omega} \left[\omega (\beta_{\parallel n} B_{\parallel\parallel} - i \beta_{\parallel b} B_{\parallel\parallel}) + \frac{1}{k_p} (\nabla_p \tilde{Z}_0) \right] \\ \epsilon_{\perp\parallel}^{(1)} &= (-\nabla_p + \beta_{\parallel n}) B_{\parallel\parallel} + i (\nabla_n + \beta_{\parallel b}) B_{\parallel\parallel} \\ &\quad + \frac{2}{\Omega} \left[\omega (\beta_{\parallel n} B_{\parallel\parallel} + i \beta_{\parallel b} B_{\parallel\parallel}) + \frac{1}{k_p} (\nabla_p \tilde{Z}_0) \right] \end{aligned}$$

$$\begin{aligned} \epsilon_{\parallel\perp}^{(1)} &= B_{\parallel\parallel} (-\nabla_n + \beta_{\parallel b}) + i B_{\parallel\parallel} (\nabla_p + \beta_{\parallel n}) \\ &\quad + \frac{2\omega}{\Omega} (\beta_{\parallel b} B_{\parallel\parallel} + i \beta_{\parallel n} B_{\parallel\parallel}) + G_{\parallel\parallel}, \\ \epsilon_{\perp\perp}^{(1)} &= (\nabla_n + \beta_{\parallel b}) B_{\parallel\parallel} + i (\nabla_p - \beta_{\parallel n}) B_{\parallel\parallel} \\ &\quad + \frac{2\omega}{\Omega} (\beta_{\parallel b} B_{\parallel\parallel} - i \beta_{\parallel n} B_{\parallel\parallel}) + G_{\parallel\parallel}. \end{aligned}$$